Quality of seepage water in a soil treated with alkali-activated cement at room temperature

Author 1

- Pedro M.S.M. Rodrigues, PhD, MSc, BSc
- Adjunct Professor, Polytechnic Institute of Guarda, Guarda, Portugal

Author 2

- Carlos Rodrigues, PhD, MSc, BSc
- Coordinator Professor, Polytechnic Institute of Guarda, Guarda, Portugal

Author 3

- Nuno Cruz, PhD, MSc, BSc
- Technical Director in Geotechnical Department of MOTA-ENGIL / Invited Professor in University of Aveiro, Portugal

Author 4

- Sara Rios, PhD, MSc, BSc, Post-Doc Research Fellow
- CONSTRUCT-GEO, Faculty of Engineering, University of Porto

Author 5

- António Viana da Fonseca, BSc, MSc. D.Eng, FIE (Port), Professor, Department of Civil Engineering
- CONSTRUCT-GEO, Faculty of Engineering, University of Porto

Abstract

Modern societies are great producers of waste because of their energy and natural resource needs. Many of these wastes are disposed of in landfills, which require a significantly-sized area of soil and special geotechnical conditions. The reaction between alumina-silicate, with an aqueous alkali hydroxide and silicate solution produces an Alkali-Activated Cement (AAC). The use of AAC, an inorganic material with a chemical structure of polymeric Si–O–Al bonds, can promote the stabilisation and immobilisation of a wide variety of waste sources containing hazardous materials. The purpose of this study is to evaluate the effect of curing conditions on the resistance, permeability and in the quality of the seepage water generated over time in transport infrastructure platforms built with soil stabilised with AAC. The strength results show that the material meets the requirements for use in building low cost roads. Permeability tests of AAC samples show a relatively low permeability (between 10^{-8} to 10^{-7} m/s), a positive factor for environmental and geotechnical considerations. However, this permeability still results in significant leachate water with quality and contaminant issues, especially in Cr, Cd, Al, Na, Si, and high pH.

1 Introduction

2 Since the middle of the last century, the growth of the world population has induced an increase

3 of waste production and a demand for energy and natural resources (Costa et al., 2010; Patrício

4 et al., 2016). As a consequence, industry and power plants face the problem of industrial wastes

5 and carbon dioxide emissions that are generated during manufacturing processes and the

6 production of energy. The quantities of industrial waste generated are enormous, many of them

7 classified as hazardous, which implies the use of large areas of land for the construction of

8 landfills. This solution is not environmental friendly and is quite expensive, not only in

9 construction but also in operation (Scheetz et al., 1999; Scharff, 2014; Camobreco et al., 1999).

10 Coal-firing power plants are one of the largest producers of fly ash (FA). FA is a hazardous

11 material which needs a disposal in industrial landfills, with the possibility of environmental

12 deterioration of waters and soils. In recent decades, efforts have been made for the application

13 of FA in civil engineering structures. For example, the application of this waste materials in

14 alkali-activated cement (AAC) can be a more environmentally sustainable solution, not only

15 because of increased recycling and use of wastes in the manufacture of new products, but also

16 because it increases the lifetime of landfills. AAC, an inorganic material with Si–O–Al links, can

17 be obtained from the chemical blend of alumina-silicate oxides with alkali and silicates at

18 temperatures under 100 ºC (Davidovits, 1991; Mehta and Siddique, 2016; Yuan et al., 2016;

19 Salahuddina et al., 2015). AAC can also promote the solidification, stabilization and

20 immobilization of a wide variety of waste sources containing heavy metals. During the curing

21 time, the reactions inside the mixture include mineral dissolution, polycondensation and

22 structural re-organization of the chemical species that are present (Phair and Van Deventer,

23 2001; Sarkar et al., 2015). AAC can also contribute to stabilizing and immobilizing heavy metals

24 and radioactive waste, decreasing their bioavailability. The effective immobilization of heavy

25 metals and other harmful compounds allows the AAC to be used in the construction industry

26 and for paving roads (Van Jaarsveld et al., 1997; Santa et al., 2016; Komnitsas, 2011).

27 In recent decades, AAC based on FA has attracted the industrial interest of power plants

28 because environmental regulations promote the use of recycled materials to lower the

29 consumption of natural resources and the decrease of carbon dioxide emission (Davidovits,

30 2005; Turner and Collins, 2013; Heath et al., 2014). This solution has important advantages,

31 such as cost, flexibility and availability of the waste FA for use as raw material. AAC has other

32 properties that make it attractive for cementation, such as long-term durability, high compressive

33 strength, high acid resistance and fast hardening (Singh et al., 2015). A typical FA-based AAC

34 blend consists, approximately, of 60% fly ash, 12% Al source and the rest alkali silicate solution

35 by mass (Swanepoel and Strydom, 2002; Van Jaarsveld et al., 1999; Yun-Ming et al., 2016).

36 The purpose of this study is to evaluate the effect of different curing conditions in the resistance

37 and permeability of an AAC and in the quality of the seepage water generated over time.

38

39 **2. Materials and Methods**

40 *2.1. Materials*

41 The results presented in this paper concern the stabilization of a Colombian soil classified as a

42 silty sand (SM), according to the unified classification system ASTM D2487 (2017). The soil was

43 collected at a quarry site called "El Cajón de Copérnico", located in Soacha in the south of

44 Bogotá, Colombia (4°33'14.5"N 74°12'21.9"W). It is a crushed sandstone mainly composed by

45 quartz and a minor quantity of muscovite with the following grading characteristics: D_{50}=0.20

46 mm, Uniformity Coefficient C_u= 200, Curvature Coefficient C_c=8.6 and fines content (D<0.074

47 mm) = 27.9%.

48 The FA used in the alkaline activation was produced by a Portuguese coal-fired thermo-electric

49 power plant, Pegop - Energia Eléctrica SA (39°28'00.7"N 8°06'52.0"W), classified as Class F

50 due to its low calcium content, according to ASTM C618 (2017). The alkaline activator solution

51 was produced mixing a sodium silicate (SS) solution with a sodium hydroxide (SH) solution

52 prepared to the desired concentration by dissolving sodium hydroxide pellets in water. The SS

53 solution has a bulk density of 1.464 g/cm^3 at 20 ºC, a SiO_2/Na_2O weight ratio of 2.0 (molar ratio

54 of 2.063) and a Na_2O concentration in the solution of 13.0%. The SH pellets have a specific

55 gravity of 2.130 at 20 ºC (99 wt %).

56

57 *2.2. Testing procedures*

58 For pH determinations, a pH meter (Tritralab TIM900, Radiometer) and a sensor (PHC3185-67,

59 Radiometer) were used and calibrated with standard solutions of pH 4.005±0.010, 7.000±0.010

60 and 10.012±0.010 (Radiometer analytical). Electrical conductivity was measured with a

conductivity meter (model 150, Orion) and a sensor (model 012210, Orion) calibrated with a 12.85±0.35% mS/cm conductivity standard (Radiometer analytical). Concentrations of major and trace elements, in the soil, ash, percolation water and circulation water (tap water) were determined by atomic absorption spectroscopy (906 model, GBC) with flame and electro-thermal (GF3000, GBC) atomizer systems. Standard solutions (Johson Mathey GmbH) were used for calibration, with a concentration of 1000 µg/ml of each element at 5% HNO_3, with the exception of aluminium, chromium and nickel solutions, which had 5% HCl.

Scanning Electron Microscopy (SEM) was performed on a Quanta SEM 400 (FEI, inc.) in low vacuum mode (1.3 mbar). The Energy Dispersive Spectroscopy (EDS) was acquired for about 10 minutes using an EDAX equipment. A dead time of 33%, with about 2,000 counts per second and a life span of 500 s was used. The quantitative analysis was carried out with the ZAF standardless model. The SEM/EDS analysis was carried out at the Electronic Microscopy Unit (UME) of the UTAD University in Vila Real, Portugal.

2.3. Composition of the mixtures and specimen preparation

The definition of the compaction properties of the mixtures was based on modified Proctor tests on specimens of soil, fly-ash and water. In this case, a fly-ash percentage of 10% of the mass of dry soil was considered because this was the selected amount used in the following mixtures. Since Proctor tests give compaction parameters of the treated soil immediately after mixing, i.e. without curing, it was considered that the presence of the activator was not very relevant and so the tests were performed with water.

Three types of mixtures were prepared as expressed in Table 1, where the water content and the dry unit weight correspond to the optimum pointed obtained in the Proctor test. Two ratios of sodium silicate/sodium hydroxide, in weight, were considered (0.5 and 1.0), as well as two different concentrations of sodium hydroxide (7.5 and 12.5 M). Each mixture was identified as follows: the letter A corresponds to the fly ash content; the number that follows the letter A, 0.5 or 1, corresponds to the SS/SH ratio, and the number following the letter C, 7 or 12, corresponds to the NaOH concentration (7.5 or 12.5 M).

The mixture was prepared by mixing the necessary quantities of soil, fly ash, sodium silicate solution, sodium hydroxide pellets and tap water, at room temperature. Since dissolution of SH

3

91   pellets in water is a highly exothermic reaction, the solution was prepared on the day before to

92   allow sufficient time to cool down to room temperature. On the moulding day, the soil and fly ash

93   were first mixed until the mixture reached completed homogenization, then the activator solution

94   (SS and SH) was added. Finally, the solids (soil and fly ash) were mixed with the alkaline

95   solution, in an electric mortar mixer, until a homogeneous paste was obtained (more or less 8

96   minutes).

97   The mixture was then statically compacted in a lubricated stainless-steel mould trying to

98   reproduce the results obtained from the Proctor test (γ_{dmax}=19.92 kN/m^3 and w_{opt}=8.0%). The

99   final dimensions of the specimens were 100 mm in diameter and 37 mm in height. The standard

100 ASTM D1632 (2017) was used as a guide for the preparation of the specimens. At the end of

101 preparation, the specimens were removed from the mould and their weight, height and diameter

102 were carefully measured. Then the specimens were placed in a climatic chamber for curing for

103 28, 60 and 90 days. This chamber was used to simulate the environmental conditions of

104 Bogotá, provided by the Facultad de Ciencias Agropecuarias – Universidad de Ciencias

105 Aplicadas e Ambientales (AGROP-UDCA) University Climatological Station. Table 2 shows the

106 data recovered over 23 years (1989-2012), where each value corresponds to a monthly average

107 of relative humidity (R_H %) or temperature (T: ºC). In that sense, environmental conditions

108 created in the climatic chamber for one day of curing correspond to a one-month average

109 climate. During one day in the chamber, the specimens were subjected, in the first 12 hours, to

110 the maximum temperature and minimum humidity and in the remaining 12 hours, to the

111 minimum temperature and maximum humidity. This means that values around 12-13 ºC are

112 much lower than the curing temperatures generally reported in the literature as room

113 temperature (Sukmak et al., 2013; Zhang et al., 2013; Phummiphan et al., 2016). After curing,

114 the specimens were subjected to unconfined compression strength tests (UCS), permeability

115 tests in triaxial chamber (K) and chemical analysis. The seepage water from the permeability

116 tests was also used in the chemical analysis. The UCS test was done exactly in the day after

117 curing and it didn´t take long (around 15 min), the permeability test was performed in the same

118 conditions of the UCS tests and it took around 7 hours. The chemical analysis took more or less

119 three weeks.

120

121 **3. Results**

122 *3.1. SEM and EDS measurements*

123 SEM photomicrograph and EDS microstructure of the fly ash and soil are shown in Figure 1. Fly

124 ash is composed of small particles with diameters between 3 and 40 μm. Many particles have a

125 random shape, distinguishing several spherical particles with diameters above 20 μm. Particle

126 size distribution analysis was carried out by measuring 126 particles, where the statistical

127 results show a minimum size of 3.72 μm, a maximum of 44.51 μm and a mean of 11.64 μm. The

128 distribution of the particle sizes in the fly ash is of bimodal type, with peaks at 7-9 μm and at 19

129 μm. The EDS analysis shows that the chemical composition of the fly ash (% by weight), on

130 average, is 53.7% Si, 19.9% Al and 11.8% Fe. The other chemical elements present are in a

131 concentration between 0.5% and 4.2%. This is similar to the typical class F Fly ash that includes

132 Si, Al and Fe over 70 wt.% and Ca less than 10 wt.%, in amorphous and crystalline oxide forms.

133 Chemical composition of the soil (% by weight) shows a predominance of Si (80.35%), Al

134 (11.4%), Fe (3.6%) and K (2.8%). Concentrations below 1% are found for Mg, P, Ti and Cu.

135 Figure 2 shows the SEM and EDS measurements of the mixtures A05C7, A05C12, and A1C7

136 (compositions in Table 1) after 1 year of curing time. The SEM images show the typical spheres

137 of the fly ash, attacked and presenting holes. At the same time, the surface of these spheres is

138 coated with some type of material that should be the AAC. Also visible are some more or less

139 elongated crystals which should correspond to hydrated crystals of sodium silicate. As reported

140 by Rios et al. (2017), the effect of cementation is clearly seen in the SEM images. The EDS

141 analyses were done, as much as possible, on the matrix zone, as far away as possible from the

142 added inert. The matrix is composed of fly ash, sodium silicate and sodium hydroxide in varying

143 proportions, according to the composition of the mixtures set out in Table 1. Thus, it is to be

144 expected that the values of the composition in this zone, in terms of values for the fly ash,

145 increase for sodium and silicon, and decrease for aluminium. This is the case for all samples.

146

147 *3.2. Unconfined compression strength tests*

148 Unconfined compression strength tests (UCS) were performed according to ASTM D1633

149 (2017). For that purpose, an automatic load frame with displacement control was used together

150 with a 25 kN capacity load cell.

151　The soil, with 10% of ash and the 3 mixtures specified in Table 1 were subjected to unconfined

152　compression strength tests at different curing times, namely, 0 days, 28 days, 60 days and 90

153　days, to evaluate the influence of composition and curing time in the specimens' strength. Each

154　test was repeated three times to have representative results for each case. In spite of some

155　variability, the results obtained in Figure 3 indicate that all specimens show a considerable

156　increase in strength compared to unbound soil specimens, in agreement with previous research

157　(Rios et al., 2016). The scatter in the UCS results may be due to the fact that alkaline

158　activations are highly susceptible to slightly variations in the curing conditions. The void ratios in

159　each specimen were around 0.3 and 0.4.

160　Based on Figure 3, it can be concluded that there is an improvement in strength with the curing

161　time, far beyond the 28th day, usually taken as a reference period for cemented materials.

162　Furthermore, the composition that showed the best results was A1C7. Considering the

163　application of this soil stabilisation treatment in the construction of low cost roads, the results

164　indicate that it is possible to obtain soils, after treatment, with great resistance, which can

165　increase the soil strength up to ten times in the case of the best mixture.

166

167　*3.3. Permeability tests*

168　At the end of the curing time (28, 60 or 90 days) the dimensions and weight of the specimens

169　were determined. This allowed to evaluate their physical characteristics. It should be noted that

170　the degree of saturation of the specimens is not constant because this depended on the final

171　humidity cycle to which they were subjected. The main purpose of the test setup was to allow

172　the collection of water for the chemical analysis. For that reason, permeability tests were

173　performed in a triaxial chamber with 50 kPa of confining stress. The base of the specimens was

174　subjected to 10 kPa of back water pressure and the top was linked to the atmospheric pressure.

175　In the permeability tests tap water was used. The specimens had 100 mm in diameter and 40

176　mm in height. The seepage water was collected in a beaker and sent for chemical analysis. In

177　all specimens, only the first 150 ml of seepage water were collected. The permeability was

178　continued until it was observed that the laminar regime was installed, in other words, when a

179　linear relationship between discharge of water and time was observed. At these moment, the

180 permeability coefficient was measured. The results of the permeability tests are presented in
181 Table 3.
182 The specimens of compositions A1C7 and A05C12 with shorter curing time (28 days) have
183 higher void ratios than the specimens with longer curing time, 90 days and 60 days,
184 respectively. However, the specimens with higher void ratios and shorter curing time have lower
185 permeability coefficients than the specimens with more curing time and lower void ratios. The
186 results seem to indicate that the evolution of the polymerization in time must create chemical
187 bonds that reduce the empty spaces occupied by the amorphous mixture of the binder, creating
188 connection between voids which seems to lead an increase of the permeability.
189
190 **3.4. Chemical characterization of the starting materials**
191 The determination of the chemical composition of the soil, fly ash and treated soil was made
192 from an extraction with a solution of aqua regia (hydrochloric/nitric acid mixture), in accordance
193 with ISO standard 11466 (1995). After the extraction procedure, the determination of major and
194 trace ions concentrations was made by atomic absorption spectroscopy, as explained in ISO
195 standard 11047 (1998). The determination of pH and electric conductivity was performed in
196 accordance with ISO standards 10390 (2005) and 11265 (1994), respectively. The solution of
197 sodium hydroxide was prepared in the laboratory and the solution of sodium silicate was
198 purchased and both were analysed in accordance with the international standards previously
199 mentioned. The results for the natural soil, ash, sodium silicate and sodium hydroxide are
200 presented in Table 4.
201 The results show the presence of significant concentrations of K, Fe, Al and Si in the soil, while
202 in the ash the concentration is more relevant for Mg, Na, Fe, Mn and Al. The sodium silicate
203 solution has, as expected, a high concentration of Si and Na, while the sodium hydroxide
204 solution has a high concentration of Na.
205
206 **3.5. Physical and chemical characterisation of the soil treated with alkali-activated**
207 **cement**

208 The chemical analyses were also performed on the soil treated with AAC by the methods

209 explained previously, for all the compositions referred to in Table 1 and for the different curing

210 periods shown in Table 5.

211 The analysis of the A05C12 results between 28 and 90 days show that, after 90 days of curing,

212 the extraction performed on the treated material produces, with exception of Mn and Cr, a lower

213 concentration of cations (alkali and alkaline-earth metals, transition and post-transition metals)

214 when compared with results obtained after 28 days curing time. A decrease in the pH value of

215 about two pH units and of the conductivity of the extraction solution are also evident. In the

216 other two mixture compositions, A1C7 and A05C7, the reduction was not so evident in all the

217 elements because the curing time was smaller (only up to 60 days). This is in agreement with

218 the UCS test results, which showed that the evolution is still relevant for a long period.

219 Nevertheless, in both mixtures, a decrease in electric conductivity was observed with increasing

220 curing time. For the pH value, the variation with the curing time was not significant. The results

221 seem to indicate that the most favourable mixture for fixing the metal ions is the composition of

222 A05C12 (with SS/SH equal to 0.5 and an SH concentration of 12.5M) and a curing time of 90

223 days. The main reason may be the greatest curing time and not the chemical composition of the

224 AAC mixture.

225 Taking into account the composition of each geopolymer produced and the chemical analyses

226 of each component used in the production of those specimens, the theoretical concentration of

227 each chemical element in the specimen was determined. The comparison between the theory

228 and the concentrations really determined in each specimen is evidence that, for most chemical

229 elements, the determined concentration is lower than the theoretical expectation. This fact

230 highlights the formation of a structure capable of fixing most chemicals present in the

231 components used to produce each specimen of AAC.

232

233 ***3.6. Chemical characterisation of the seepage water***

234 For the application of AAC in some engineering work, such as road/pavement structures or

235 landfills, it is important to verify the potential environmental impact of these materials. Table 6

236 presents the results of the chemical analysis of circulation water (tap water) and seepage

237 waters, from the permeability tests, for the three different specimen compositions, with different

238   curing times. The tap water used in the tests has substantially lower concentrations than those

239   found in seepage water, especially for the transition and post-transition metals. For the alkaline-

240   earth metals, namely for calcium and magnesium, the concentrations in the tap water are higher

241   than in the seepage water, which seems to indicate that these cations are retained in the matrix

242   of the soil treated. The results of the seepage water, in general, show that the concentration of

243   the chemical elements, as well as the pH and electrical conductivity, decrease with increasing

244   curing time. Similar results are obtained in the chemical characterization of the treated soil

245   presented above in section 3.5. A higher concentration of sodium in the seepage water of

246   A05C12, relative to the other compositions, is due to the fact that, in the first case a sodium

247   hydroxide solution with a concentration of 12.5 M was used, while in the others, a concentration

248   of 7.5 M was used. On the other hand, taking into account the silicate concentration in the

249   seepage water, the molar ratio of SS/SH equal to 0.5, used in the preparation of the AAC,

250   appears to be more favourable than the molar ratio of 1.

251   The same conclusions are obtained if the evolution of the metals concentration with curing time

252   is compared, as presented in Figure 4. For the majority of chemical parameters measured

253   during the tests, a decrease of the concentration with increasing curing time is observed, which

254   may also be attributed to the establishment of a larger number of chemical bonds in the AAC

255   structure, or to the effect of leaching between trials. Indeed, the aluminosilicate network

256   structure is formed when fly ash comes into contact with NaOH, Si, Al, and other species are

257   released and transfer. The transfer of Al and Si species and the condensation of aluminosilicate

258   oligomers have an effect on the growth and the charge density of the chain, the rate, and the

259   extent of polymerization. At room temperature this process is slower, and then the chemical

260   species, like Si or Al, are more available to become leachate. On the other hand, hazardous

261   elements, such as Zn, Mn, Cr, Cd, Ni, or Pb can be immobilized by physical encapsulation and

262   chemical stabilization in the three-dimensional structure of the geopolymer matrix. While this

263   network is still not formed, or stabilized, these elements can be easily removed.

264   From an environmental point of view, it is evident that the seepage water has very high amounts

265   of sodium, aluminium and silica, as well as a high pH. These values can threaten the natural

266   ecosystems. Since this is, to a large extent, a result of the addition of sodium hydroxide and

267   sodium silicate, it may be possible to minimize the environmental impact by adjusting the

268   concentration of the different components at the time of AAC preparation. In particular, mixtures

269   that have shorter curing periods or that can achieve greater strength at an early age may have

270   better leaching behaviour. As noted earlier, it is highly unlikely that all the silica, sodium,

271   aluminium and other chemical elements of the mixtures analysed take part in the synthesis

272   reaction of the AAC. Since much better results have been found by other researchers working

273   with AAC without soil (Phair et al., 2004), it is possible that more AAC is necessary for the same

274   amount of soil. This will increase the bonding between particles, which may reduce permeability

275   and, consequently, leaching. Another important fact that may contribute to the contamination of

276   the seepage water is the inclusion of impurities in the chemical composition of AAC raw

277   materials. Calcium and iron from fly ash has the effect of adding reaction pathways during

278   polymerization. These side reactions can cause big changes in the material properties during

279   the synthesis and in the final product as pointed out by Duxson et al. (2007). Furthermore, it is

280   recognized that the properties of alkali-activated materials are highly dependent on the curing

281   conditions (Criado et al., 2005; Izquierdo et al., 2010), especially on the curing temperature

282   (Palomo et al., 1999; Andini et al., 2008). Considering that these tests were performed at a

283   relatively low temperature (around 13 ºC) it is possible that the results were significantly affected

284   by this condition.

285   If the seepage water quality is compared with the emission limit value (ELV) for the wastewater

286   in the Portuguese decree-law (DL No. 236/98) (Portuguese law, 1998), there are some values

287   associated to elements such as cadmium, chromium and aluminium that go over the limit

288   values.

289

290   **4. Conclusions**

291   The mixture compositions for soil stabilization in transport infrastructure platforms that were

292   analysed showed very significant strength improvements in comparison with the initial soil.

293   As might be expected, curing time promotes the improvement of these properties. However,

294   comparing strength results of similar specimens (the same compositions and the curing time),

295   but with different conditions of temperature and humidity, a significant influence of these

296   parameters was found. This can be explained by the great sensitivity of alkaline activation

297   reactions to temperature and humidity conditions during curing.

298   For this type of soil and water used in the experiments, the permeability tests showed relatively

299   low values (between 10^{-8} to 10^{-7} m/s). This is a positive factor for the treatment of landfills with

300   alkaline binders as it assures a better encapsulation of waste materials that constitute the

301   binder. However, this value is not null and the seepage water quality revealed a chemical

302   composition with an important environmental risk. In fact, the comparison between the emission

303   limit values, listed in Portuguese law No. 236/98 (see also Directive 2000/60/EC) (EU, 2000),

304   and the measured values in the seepage waters in the different samples indicate the existence

305   of prohibited concentrations, namely those relating to the elements cadmium, chromium, and

306   aluminium as well as pH level. High concentrations of sodium and silicon were also detected,

307   which can have an important effect in the balance of the natural ecosystems.

308   In summary, the application of a soil stabilization technique with wastes for transport

309   infrastructure platforms is a good technical and environmental solution, which necessarily

310   requires new studies to adapt the composition or the curing conditions in order to minimize the

311   environmental impact without reducing the geotechnical properties.

312   Finally, new studies will be developed to understand how the concentration of leached elements

313   behaves in time and to determine the consequences to the mechanical structure.

314

326

327   **References**

328   Andini S, Cioffi R, Colangelo F et al. (2008) Coal fly ash as raw material for the manufacture of

329   geopolymer-based products. Waste Management 28: 416-423,

330   https://doi.org/10.1016/j.wasman.2007.02.001.

331   ASTM (2017a) D2487-17, Standard Practice for Classification of Soils for Engineering Purposes

332   (Unified Soil Classification System). ASTM International, West Conshohocken, PA, USA.

333   ASTM (2017b) C618-17a, Standard Specification for Coal Fly Ash and Raw or Calcined Natural

334   Pozzolan for Use in Concrete. ASTM International, West Conshohocken, PA, USA.

335   ASTM (2017c) D1632-17, Standard Practice for Making and Curing Soil-Cement Compression

336   and Flexure Test Specimens in the Laboratory. ASTM International, West Conshohocken,

337   PA, USA.

338   ASTM (2017d) D1633-17, Standard Test Methods for Compressive Strength of Molded Soil-

339   Cement Cylinders. ASTM International, West Conshohocken, PA, USA.

340   Camobreco V, Ham R, Barlaz M et al. (1999) Life-cycle inventory of a modern municipal solid

341   waste landfill. Waste Management Research **17**: 394-411, https://doi.org/10.1034/j.1399-

342   3070.1999.00079.x.

343   Costa I, Massard G and Agarwal A (2010) Waste management policies for industrial symbiosis

344   development: case studies in European countries. Journal of Cleaner Production **18**: 815-

345   822, http://dx.doi.org/10.1016/j.jclepro.2009.12.019.

346   Criado M, Palomo A and Fernández-Jiménez A (2005) Alkali activation of fly ashes. Part 1:

347   Effect of curing conditions on the carbonation of the reaction products. Fuel **84**: 2048-2054,

348   http://dx.doi.org/10.1016/j.fuel.2005.03.030.

349   Davidovits J (1991) Geopolymers: inorganic polymeric new materials. Journal of Thermal

350   Analysis **37**: 1633-1656, http://dx.doi.org/10.1007/BF01912193.

351   Davidovits J (2005) Geopolymer, Green chemistry and sustainable development Solutions. The

352   poly(sialate) terminology: a very useful and simple model for the promotion and

353   understanding of green-chemistry. In *Proceedings of the World Congress Geopolymer* (J.

354   Davidovits (Ed.)). Saint-Quentin, France, pp. 9-15.

355   Duxson P, Fernández-Jiménez A, Provis J et al. (2007) Geopolymer technology: the current

356   state of the art. Journal of Materials Science 42: 2917-2933. https://doi.org/10.1007/s10853-

357   006-0637-z.

358   Heath A, Paine K and McManus M (2014) Minimising the global warming potential of clay based

359   geopolymers. Journal of Cleaner Production 78: 75-83,

360   https://doi.org/10.1016/j.jclepro.2014.04.046.

361   ISO (1994) 11265:1994. Soil quality – Determination of the specific electrical conductivity.

362   International Organization for Standardization, Genève, Switzerland.

363   ISO (1995) 11466:1995. Soil quality – Extraction of trace elements soluble in aqua regia.

364   International Organization for Standardization, Genève, Switzerland.

365   ISO (1998) 11047:1998. Soil quality – Determination of cadmium, chromium, cobalt, copper,

366   lead, manganese, nickel and zinc – Flame and electrothermal atomic absorption

367   spectrometric methods. International Organization for Standardization, Genève, Switzerland.

368   ISO (2005) 10390:2005. Soil quality - Determination of pH. International Organization for

369   Standardization, Genève, Switzerland.

370   Izquierdo M, Querol X, Phillipart C et al. (2010) The role of open and closed curing conditions

371   on the leaching properties of fly ash-slag-based geopolymers. Journal of Hazardous

372   Materials **176**: 623-628, https://doi.org/10.1016/j.jhazmat.2009.11.075.

373   Komnitsas K (2011) Potential of geopolymer technology towards green buildings and

374   sustainable cities. Procedia Engineering **21**: 1023-1032,

375   https://doi.org/10.1016/j.proeng.2011.11.2108.

376   Mehta A and Siddique R (2016) An overview of geopolymers derived from industrial by-

377   products. Construction and Building Materials **127**: 183-198,

378   http://dx.doi.org/10.1016/j.conbuildmat.2016.09.136.

379   Palomo A, Grutzeck M and Blanco M (1999). Alkali-activated fly ashes: A cement for the future.

380   Cement and Concrete Research **29**: 1323-1329, https://doi.org/10.1016/S0008-

381   8846(98)00243-9.

382   Patrício J, Costa I and Niza S (2016). Urban material cycle closing e assessment of industrial

383   waste management in Lisbon region. Journal of Cleaner Production **106**: 389-399,

384   https://doi.org/10.1016/j.jclepro.2014.08.069.

385   Phair J and Van Deventer J (2001) Effect of silicate activator pH on the leaching and material

386   characteristics of waste-based inorganic polymers. Minerals Engineering **14**: 289-304,

387   https://doi.org/10.1016/S0892-6875(01)00002-4.

388 Phair J, Van Deventer J and Smith J (2004) Effect of Al source and alkali activation on Pb and

389   Cu immobilisation in fly ash based geopolymers. Applied Geochemistry **19**: 423-434,

390   https://doi.org/10.1016/S0883-2927(03)00151-3.

391 Phummiphan I, Horpibulsuk S, Sukmak P et al. (2016) Stabilisation of marginal lateritic soil

392   using high calcium fly ash-based geopolymer. Road Materials and Pavement Design **17**:

393   877-891, https://doi.org/10.1080/14680629.2015.1132632.

394 Portuguese law (1998) Decreto-Lei no 236/98. D.R. I Série. 176: 3676–3722.

395 Rios S, Cristelo C, Viana da Fonseca A et al. (2016) Structural Performance of Alkali Activated

396   Soil-Ash versus Soil-Cement. Journal of Materials in Civil Engineering **28**: 1-11.

397   https://doi.org/10.1061/(ASCE)MT.1943-5533.0001398.

398 Rios S, Ramos C, Viana da Fonseca A et al. (2017) Mechanical and durability properties of a

399   soil stabilized with an alkali-activated cement. European Journal of Environment and Civil

400   Engineering, 1-23, http://dx.doi.org/10.1080/19648189.2016.1275987.

401 Salahuddina M, Norkhairunnisa M and Mustapha F (2015) A review on thermophysical

402   evaluation of alkali-activated geopolymers. Ceramics International **41**: 4272-4281,

403   https://doi.org/10.1016/j.ceramint.2014.11.119.

404 Santa R, Soares C and Riella H (2016) Geopolymers with a high percentage of bottom ash for

405   solidification/immobilization of different toxic metals. Journal of Hazardous Materials **318**:

406   145-153, https://doi.org/10.1016/j.jhazmat.2016.06.059.

407 Sarkar M, Dana K and Das S (2015) Microstructural and phase evolution in metakaolin

408   geopolymers with different activators and added aluminosilicate fillers. Journal of Molecular

409   Structure **1098**: 110-118, https://doi.org/10.1016/j.molstruc.2015.05.046.

410 Scharff H (2014) Landfill reduction experience in The Netherlands. Waste Management **34**:

411   2218-224, https://doi.org/10.1016/j.wasman.2014.05.019.

412 Scheetz B, Roy D and Grutzeck M (1999). Giga-scale disposal: a real frontier for ceramic

413   research. Material Research Innovations **3**: 55-64, https://doi.org/10.1007/s100190050125.

414 Singh B, Ishwarya G, Gupta M and Bhattacharyya S (2015) Geopolymer concrete: A review of

415   some recent developments. Construction and Building Materials **85**: 78-90,

416   https://doi.org/10.1016/j.conbuildmat.2015.03.036.

417   Sukmak P, Horpibulsuk S and Shen S (2013) Strength development in clay–fly ash geopolymer.

418   Construction   and   Building   Materials   **40**:   566-574,

419   https://doi.org/10.1016/j.conbuildmat.2012.11.015.

420   Swanepoel J and Strydom C (2002) Utilisation of fly ash in a geopolymeric material. Applied

421   Geochemistry **17**: 1143-1148, https://doi.org/10.1016/S0883-2927(02)00005-7.

422   Turner L and Collins F (2013) Carbon dioxide equivalent (CO_2-e) emissions: A comparison

423   between geopolymer and OPC cement concrete. Construction and Building Materials **43**:

424   125-130, https://doi.org/10.1016/j.conbuildmat.2013.01.023.

425   Van Jaarsveld J, Van Deventer J and Lorenzen L (1997) The potential use of geopolymeric

426   materials to immobilize toxic metals: part 1. Theory and applications. Minerals Engineering

427   **10**: 659-669, https://doi.org/10.1016/S0892-6875(97)00046-0.

428   Van Jaarsveld J, Van Deventer J and Lorenzen L (1999). The potential use of geopolymeric

429   materials to immobilise toxic metals: part II. Material and leaching characteristics. Minerals

430   Engineering **12**: 75-91, https://doi.org/10.1016/S0892-6875(98)00121-6.

431   Yuan J, He P, Jia D et al. (2016) Effect of curing temperature and SiO_2/K_2O molar ratio on the

432   performance of metakaolin-based geopolymers. Ceramics International **42**: 16184-16190,

433   https://doi.org/10.1016/j.ceramint.2016.07.139.

434   Yun-Ming L, Cheng-Yong H, Bakri M et al. (2016) Structure and properties of clay-based

435   geopolymer   cements: A   review.   Progress   in   Materials   Science   **83**:   595-629,

436   https://doi.org/10.1016/j.pmatsci.2016.08.002.

437   Zhang M, Guo H, El-Korchi T et al. (2013) Experimental feasibility study of geopolymer as the

438   next-generation   soil   stabilizer.   Construction   and   Building   Materials   **47**:   1468-1478,

439   https://doi.org/10.1016/j.conbuildmat.2013.06.017.

440

441

442   **Figure captions**

443   Figure 1. SEM image and EDS of small particles of fly ash (a1) and random shape soil particles

444   from El Cajón de Copérnico (Soacha, Colombia) (b2).

445   Figure 2. SEM image and EDS of mixtures of AAC: A05C7 coated with fly ash (a1), A05C12

446   with crystals of sodium silicate (b2) and A1C7 with crystals of sodium silicate (c3).

447 Figure 3. Unconfined compression strength tests result at 0, 28, 60 and 90 days of cure for the
448 soil, soil with 10% of ash and 3 mixtures of AAC.
449 Figure 4. Variation of Fe, Zn, Al, Si and Na in the seepage water of the following alkali-activated
450 specimens at different curing times: a) A05C12, b) A05C7 and c) A1C7.
451
452 **Table captions**
453 Table 1. Composition of the mixtures
454 Table 2. Environmental curing conditions from 21206260 C.UNIV. AGROP-UDCA, Bogotá
455 station.
456 Table 3. Results of the permeability tests.
457 Table 4. Results of chemical analyses of the extraction solutions of aqua regia for the soil, ash
458 and for the solutions of sodium silicate and sodium hydroxide (mg/kg).
459 Table 5. Results of chemical analyses in the soil treated with AAC for 3 different compositions
460 and different curing times.
461 Table 6. Chemical results of seepage waters from permeability tests for different compositions
462 and curing times.
463
464
465
466
467
468
469
470
471
472
473
474 FIGURES

475
476   Figure 1

477

478

479

480
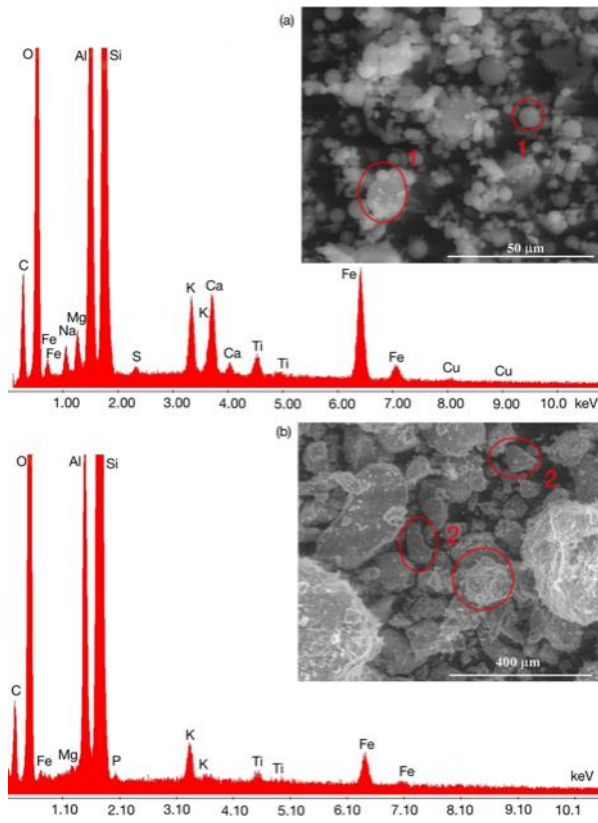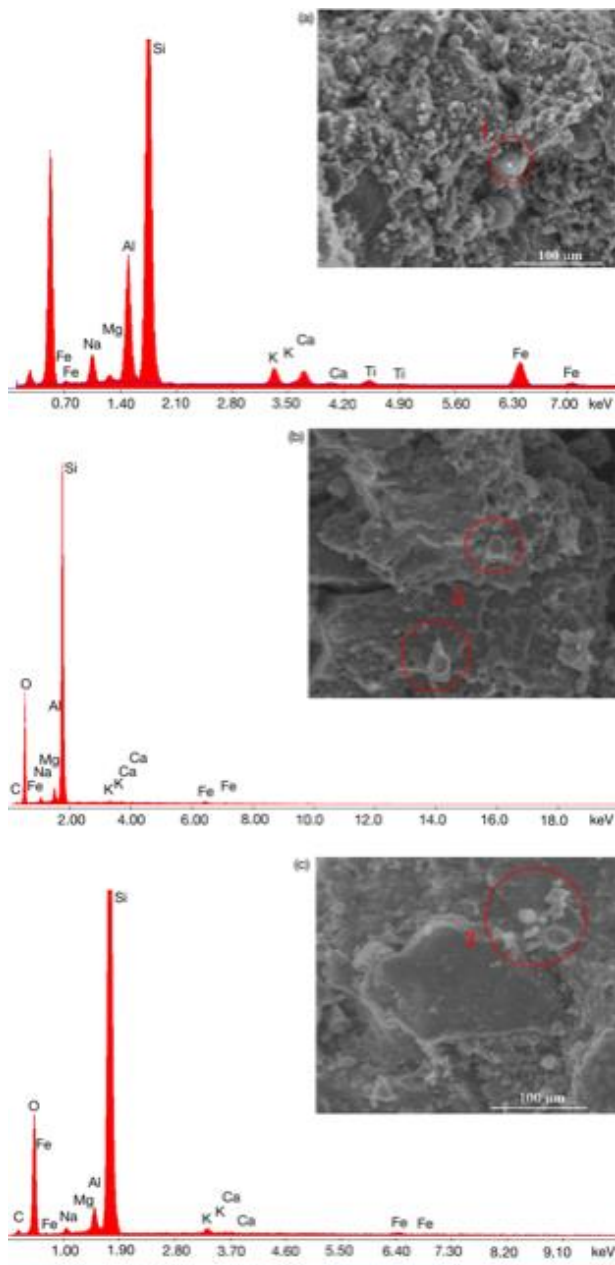
481
482 Figure 2
483
484
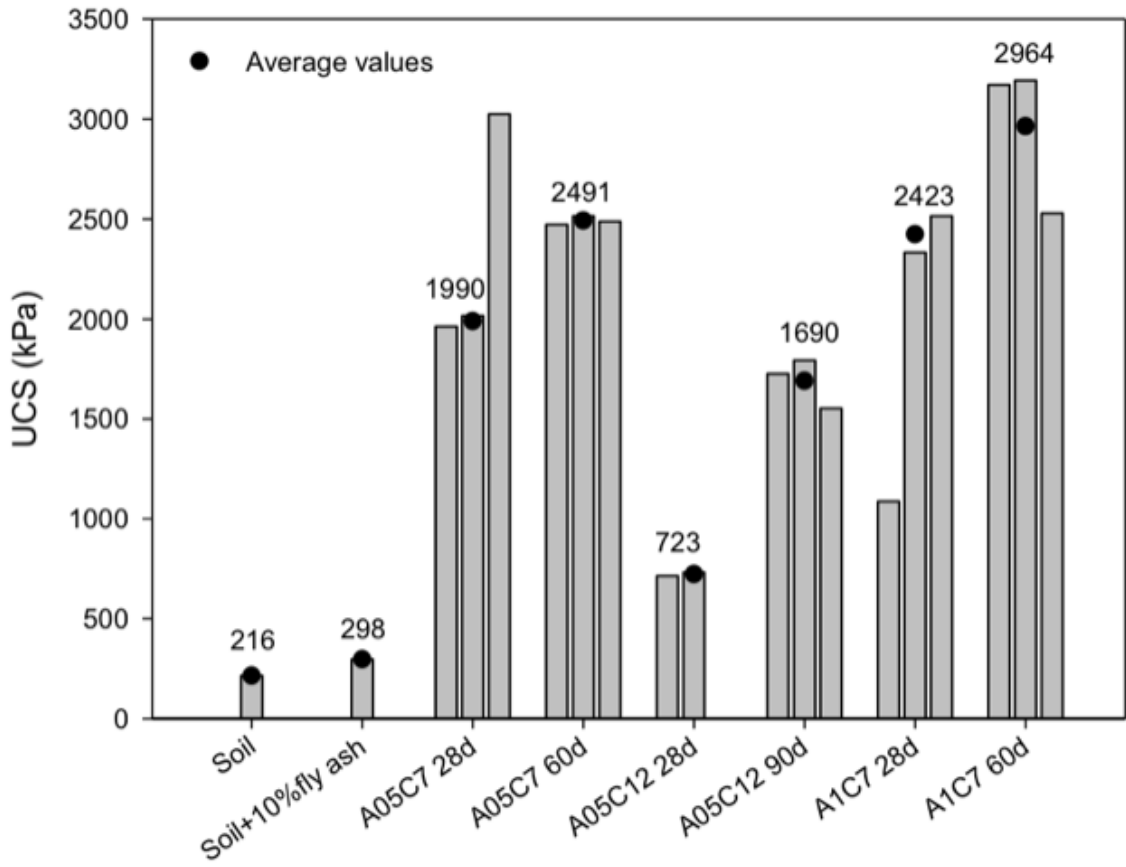
485
486   Figure 3

487
488
489
490
491

a)   b)   c)
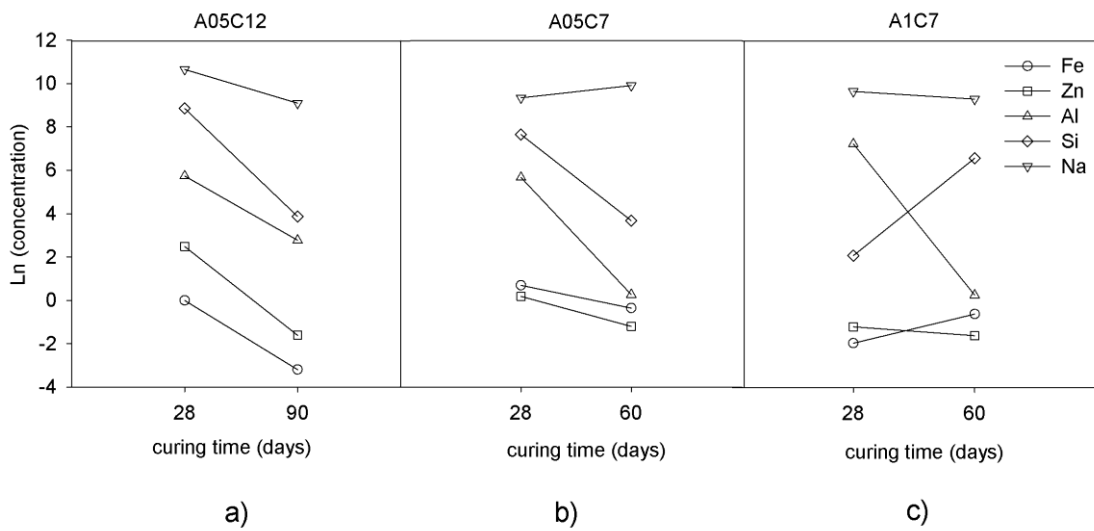
492
493   Figure 4
494

495 TABLES

496 **Table 1. Composition of the mixtures**

Name	% Fly ash	Dry unit weight (kN/m³)	Liquid content (%)	SS/SH (wt)	SH concentration (M)
A05C7	10	19.92	8.0	0.5	7.5
A05C12	10	19.92	8.0	0.5	12.5
A1C7	10	19.92	8.0	1	7.5

497
498 Table 2. Environmental curing conditions from 21206260 C.UNIV. AGROP-UDCA, Bogotá
499 station.

Month	Time	T (ºC)	RH (%)	Time	T (ºC)	RH (%)
Jan	0-12h	14.3	71	12-24h	13.0	93
Feb	0-12h	15.2	73	12-24h	13.0	94
Mar	0-12h	15.0	74	12-24h	13.2	95
Apr	0-12h	14.7	79	12-24h	12.7	95
May	0-12h	14.7	80	12-24h	13.1	95
Jun	0-12h	14.5	76	12-24h	13.1	95
Jul	0-12h	14.5	79	12-24h	13.2	94
Aug	0-12h	14.4	77	12-24h	13.0	95
Sep	0-12h	14.2	74	12-24h	12.9	94
Oct	0-12h	14.4	79	12-24h	13.0	94
Nov	0-12h	14.4	80	12-24h	13.2	95
Dec	0-12h	14.3	74	12-24h	12.6	94

500

501
502 Table 3. Results of the permeability tests.

Specimen	Days of curing	Unit weight, γ (kN/m³)	Void ratio (e)	Initial degree of saturation (S)	Permeability K (m/s)	Recording time (min)
A05C7	28	17.57	0.485	50.90	2.94E-08	81.6
	60	17.32	0.506	59.34	2.26E-07	81.8
A1C7	28	16.09	0.622	62.78	3.77E-09	129.2
	60	17.75	0.470	29.84	3.10E-07	47.2
A05C12	28	16.09	0.622	62.78	1.43E-07	188.0
	90	17.70	0.472	25.04	2.81E-07	37.7

503
504
505
506
507
508
509
510
511
512
513

514 Table 4. Results of chemical analyses of the extraction solutions of aqua regia for the soil, ash
515 and for the solutions of sodium silicate and sodium hydroxide (mg/kg).

Element	Natural soil	Ash	Na_2SiO_3	NaOH
	(mg/kg)			
K	1419	3867	17	4
Ca	19	3449	1	1
Mg	164	5051	-	2
Na	57	4060	523017	618156
Cu	19	33	6	2
Fe	5062	40259	33	4
Zn	26	79	4	3
Mn	44	443	43	1
Cr	8	47	1	3
Cd	9	11	0	8
Ni	1	131	16	22
Pb	33	27	4	16
Al	7051	31848	18	1
Si	611	321	116644	50
pH	5.3	9.5	12.8	13.2
Cond. (mS/cm)	0.8	1.9	34.4	302

516
517

518 Table 5. Results of chemical analyses in the soil treated with AAC for 3 different compositions
519 and different curing times.

Element	A05C12-28d	A05C12-90d	A1C7-28d	A1C7-60d	A05C7-28d	A05C7-60d
	(mg/kg)					
K	880	663	708	901	815	1052
Ca	83	76	60	83	72	40
Mg	651	541	539	562	599	571
Na	8555	7128	6935	5535	13840	9691
Cu	7	7	10	7	7	10
Fe	7385	7141	8085	6988	8410	7481
Zn	153	70	96	37	29	30
Mn	23	70	27	27	23	27
Cr	49	56	41	87	44	6
Cd	4	1	1	0.3	4	12
Ni	13	7	10	17	7	10
Pb	17	17	17	13	16	47
Al	11126	9566	9588	13118	9434	10435
Si	2047	1221	1383	954	1609	3153
pH	12.4	10.9	12.2	12.1	12.2	11.6
Cond. (mS/cm)	70.9	57.1	68.9	53.6	58.9	6.8

520
521
522
523
524
525
526

527 Table 6. Chemical results of seepage waters from permeability tests for different compositions
528 and curing times.

Elements	DL nº 236/98 ELV	Circulation water	A05C12 -28d	A05C12- 90d	A05C7- 28d	A05C7- 60d	A1C7- 28d	A1C7- 60d
				mg/L				
K	-	0.4	134	53	50	39.1	25	22
Ca	-	16	<0.1	2.6	0.5	0.1	0.1	0.9
Mg	-	1.5	<0.1	0.5	0.9	0.3	<0.1	0.1
Na	-	6.5	42308	8891	11604	20468	15925	11161
Cu	1.0	0.0001	4.7	0.4	1.2	0.6	1.6	0.3
Fe	2.0	0.017	1.0	0.041	2.0	0.7	0.141	0.541
Zn	-	0.2	12	0.2	1.2	0.3	0.3	0.2
Mn	2.0	0.002	0.09	0.020	0.066	0.1	0.028	0.033
Cr	2.0	0.004	5.0	2.6	1.7	0.18	1.7	1.9
Cd	0.2	0.0004	0.179	0.182	0.142	0.328	0.242	0.158
Ni	2.0	0.2	0.4	0.2	0.3	0.4	0.2	0.1
Pb	1.0	0.001	0.7	0.3	0.4	0.6	0.4	0.2
Al	10	0.3	310	16	293	1.3	1416	1.3
Si		2.4	6974	48	2132	39.7	8.1	730
pH	6.0-9.0	7.5	12.9	11.4	12.8	11.9	11.9	11.8
Cond. (mS/cm)	-	1.7	3740	695	1047	51.2	705	666

529
530